



HAL
open science

Chronic Corticosterone Elevation Suppresses Adult Hippocampal Neurogenesis by Hyperphosphorylating Huntingtin

Fabienne Agasse, Indira Mendez-David, Wilhelm Christaller, Rémi Carpentier, Barbara Y. Braz, Denis J. David, Frédéric Saudou, Sandrine Humbert

► **To cite this version:**

Fabienne Agasse, Indira Mendez-David, Wilhelm Christaller, Rémi Carpentier, Barbara Y. Braz, et al.. Chronic Corticosterone Elevation Suppresses Adult Hippocampal Neurogenesis by Hyperphosphorylating Huntingtin. *Cell Reports*, 2020, 32, pp.107865 -. 10.1016/j.celrep.2020.107865 . hal-03491369

HAL Id: hal-03491369

<https://hal.science/hal-03491369>

Submitted on 18 Jul 2022

HAL is a multi-disciplinary open access archive for the deposit and dissemination of scientific research documents, whether they are published or not. The documents may come from teaching and research institutions in France or abroad, or from public or private research centers.

L'archive ouverte pluridisciplinaire **HAL**, est destinée au dépôt et à la diffusion de documents scientifiques de niveau recherche, publiés ou non, émanant des établissements d'enseignement et de recherche français ou étrangers, des laboratoires publics ou privés.



Distributed under a Creative Commons Attribution - NonCommercial 4.0 International License

Chronic corticosterone elevation suppresses adult hippocampal neurogenesis by hyperphosphorylating Huntingtin

Fabienne Agasse¹, Indira Mendez-David^{2,3}, Wilhelm Christaller^{1,3}, Rémi Carpentier^{1,3}, Barbara Y. Braz¹, Denis J. David², Frédéric Saudou¹ and Sandrine Humbert^{1,*}

¹Univ. Grenoble Alpes, Inserm, U1216, CHU Grenoble Alpes, Grenoble Institut Neurosciences, 38000 Grenoble, France

²Université Paris-Saclay, Centre de recherche en Epidémiologie et Santé des Populations (CESP), Inserm, Faculté de Pharmacie, 92290 Châtenay-Malabry, France

³Contributed equally

*Correspondence:

Sandrine Humbert

Grenoble Institut des Neurosciences, Inserm U1216, UGA

Bâtiment Edmond J. Safra

Chemin Fortuné Ferrini

38700 La Tronche, France

Phone: +33(0)4 56 52 06 29

Email: sandrine.humbert@univ-grenoble-alpes.fr

Lead Contact, Sandrine Humbert

sandrine.humbert@univ-grenoble-alpes.fr

SUMMARY

Chronic exposure to stress is a major risk factor for neuropsychiatric disease, and elevated plasma corticosterone (CORT) correlates with reduced levels of both brain-derived neurotrophic factor (BDNF) and hippocampal neurogenesis. Precisely how these phenomena are linked, however, remains unclear. Using a cortico-hippocampal network-on-a-chip, we find that the glucocorticoid receptor agonist dexamethasone (DXM) stimulates the cyclin-dependent kinase 5 (CDK5) to phosphorylate huntingtin (HTT) at serines 1181 and 1201 (S1181/1201), which retards BDNF vesicular transport in cortical axons. Parallel studies in mice show that CORT induces phosphorylation of these same residues, reduces BDNF levels, and suppresses neurogenesis; the adverse effects of CORT are reduced in mice bearing an unphosphorylatable mutant HTT (*Hdh^{S1181A/S1201A}*). The protective effect of unphosphorylatable HTT, however, disappears if neurogenesis is blocked. The CDK5-HTT pathway, which regulates BDNF transport in the cortico-hippocampal network, thus provides a missing link between elevated corticosterone levels and suppressed neurogenesis.

Keywords: neurogenesis, corticosterone, Huntingtin, CDK5, depression, BDNF, axonal transport.

INTRODUCTION

In both rodents and humans, the hippocampus generates new neurons throughout the lifespan. This ongoing activity is particularly susceptible to environmental and experiential input such as stress (Kempermann et al., 2018). Normal adult hippocampal neurogenesis correlates with learning, memory, and mood regulation, and confers resilience to stress-induced depression (Anacker et al., 2018)—yet chronic stress in humans and animals, which causes elevated levels of cortisol (or corticosterone), can suppress neurogenesis and reduce hippocampal volume (Bremner et al., 2000; Schoenfeld et al., 2017; Vyas et al., 2016). What determines which side of this bi-directional relationship carries more weight is a mystery, though the balance can be tipped: antidepressants such as fluoxetine exert their benefits by restoring hippocampal neurogenesis and increasing levels of Brain-derived Neurotrophic Factor (BDNF), which promotes neuronal maturation, dendritic growth and synaptic transmission in the hippocampus (Boldrini et al., 2012; Boldrini et al., 2009; Chan et al., 2008; Chen et al., 2001; Santarelli et al., 2003). The precise molecular mechanisms and neural circuits underlying these influences, however, have remained elusive.

Many studies have sought to understand how BDNF functions in the stress response and in the pathophysiology of depression. In depressed patients, both BDNF levels and neurogenesis are diminished (Huang et al., 2008). BDNF is normally secreted by dentate gyrus neurons to stimulate neurite growth and ramification (Wang et al., 2015; Waterhouse et al., 2012); it also enters the hippocampus from the entorhinal cortex, which is the primary source of input fibers to the hippocampus *via* the perforant path (Kang and Schuman, 1995). Interestingly, stimulation of the entorhinal cortico-hippocampal circuit mitigates depression-like symptoms in mice under conditions of chronic stress by increasing hippocampal neurogenesis (Brüel-Jungerman et al., 2006; Stone et al., 2011; Yun et al., 2018), but whether or how BDNF is involved in this antidepressant effect remains unknown. The molecular mechanisms regulating BDNF distribution in the cortico-hippocampal circuit under conditions of stress have yet to be discovered.

Here, we sought to delineate the effects of chronically elevated corticosterone levels on BDNF distribution in the cortico-hippocampal circuit in mice. Since studying

the kinetics of BDNF vesicles in projecting axons *in vivo* is not yet possible, we used microfluidic devices to recreate mature neuronal circuits (Virlogeux et al., 2018) in a close-to-physiological context in order to study axonal transport. We then studied the consequences of corticosterone-influenced BDNF transport on neurogenesis *in vivo*.

RESULTS

Corticosteroid slows cortical transport of BDNF in a cortico-hippocampal neuronal network

To test *in vitro* whether stress affects cortical delivery of BDNF to the hippocampus, we reconstructed cortico-hippocampal neuronal networks on silicone-based micro-chips (Figures 1A and 1B). Because the E15.5 embryonic entorhinal cortex on its own provides an insufficient number of cells for culturing, we dissected out whole cortices, which consist of 25% reelin-positive neurons, i.e., cells expressing the chemical type displayed by layer II neurons of the entorhinal cortex that project to the dentate gyrus (DG) (Figure S1A) (Witter et al., 2017). We plated the cortical and hippocampal neurons in the presynaptic and the postsynaptic compartments, respectively and allowed the cellular network to mature for seven days (Virlogeux et al., 2018). By this time, most of the connections are oriented, and Tau-positive cortical axons establish synapses with MAP2-positive hippocampal dendrites within the synaptic compartment (Figure 1B).

To mimic the systemic increase of corticosterone that occurs with chronic stress, we applied the glucocorticoid receptor agonist dexamethasone (DXM, 5 μ M) to both presynaptic and postsynaptic chambers three hours before imaging with spinning disk confocal microscopy. We recorded vesicular trafficking in the distal part of the micro-channels containing the cortical axons, generated kymographs from the videos, and measured the velocity and numbers of BDNF-carrying vesicles moving in anterograde or retrograde directions (Figure 1C). DXM treatment slowed the anterograde transport of BDNF vesicles in WT cortical axons (Mann-Whitney test, $**p < 0.01$) (Figure 1C) without affecting the overall number of vesicles moving within axons. This indicates that DXM affects the transport of BDNF rather than its production.

To account not only for the velocity of the vesicles but also their number and

direction of movement relative to soma/axon terminal orientation, we also calculated the net flux (Virlogeux et al., 2018). A positive value would indicate more BDNF moving from the soma to the terminals. DXM treatment significantly reduced the net flux of BDNF (Mann-Whitney test, $*p < 0.05$) (Figure 1C).

Corticosterone augments CDK5 phosphorylation of Huntingtin

To investigate the mechanisms by which DXM reduces BDNF vesicular transport, we considered molecular motors and adaptors, which determine the efficiency and directionality of transport (Hirokawa et al., 2010). Axonal transport of vesicular BDNF relies on huntingtin (HTT), which serves as a scaffold for motor protein complexes (Gauthier et al., 2004; Saudou and Humbert, 2016). Because stress has been shown to upregulate activity of the serine-threonine kinase cyclin-dependent kinase 5 (CDK5) in the mouse cortex (Papadopoulou et al., 2015), we examined HTT phosphorylation at serines 1181 and 1201, which is accomplished by CDK5 (Ben M'barek et al., 2013).

We found that treating cortical neurons with DXM increased phosphorylation of both serine 1181 and 1201 ($**p < 0.01$, Mann-Whitney test), as measured by antibodies specific to these serines when they are phosphorylated (Ben M'barek et al., 2013)(Figures 1D and S1B). DXM also increased cleavage of p35 into p25, the constitutive activator of CDK5 ($*p < 0.05$). The CDK5 inhibitor roscovitine hindered DXM-mediated phosphorylation (Figure 1D), whereas over-activation of CDK5 by transfecting neurons with p25 increased HTT phosphorylation of both serine 1181 and 1201 ($*p < 0.05$ and $**p < 0.01$, respectively) (Figures 1E and S1C).

We therefore examined the consequences of CDK5 over-activation on vesicular transport. We found that p25 reduced the anterograde velocity and the net flux of BDNF vesicles by approximately 15% and 65%, respectively ($*p < 0.05$, Mann-Whitney test) (Figures 2A and S1C). Cortical neurons expressing a kinase-dead form of CDK5 (CDK5-KD) and treated with either DXM or DMSO showed no change in BDNF transport with DXM (Figures 2B and S1C); neither p25 nor CDK5 had any effect on the number or the net flux of moving vesicles. Thus, DXM requires CDK5 activation in order to slow BDNF transport.

To determine whether the effects of DXM and p25 on BDNF transport are mediated

by HTT phosphorylation, we reconstituted a cortico-hippocampal network using neurons from *Hdh*^{S1181A/S1201A} embryos, which lack phosphorylation at S1181/1201 (Ben M'barek et al., 2013). DXM had no effect on the anterograde velocity of BDNF vesicles in *Hdh*^{S1181A/S1201A} neurons (Figure 2C), nor did hyper-activation of CDK5 by p25 (Figure 2D). Thus, in the absence of HTT phosphorylation at S1181/S1201, neither DXM nor p25 is able to slow the anterograde transport of BDNF. We conclude that DXM-mediated stress response alters BDNF transport *via* the CDK5-HTT pathway.

Corticosterone induces phosphorylation of HTT at CDK5 sites *in vivo*

We next asked whether chronic administration of low-dose CORT—5 mg/kg/day, administered to WT mice for at least four weeks (David et al., 2009) to mimic chronic stress—induces HTT phosphorylation by CDK5 *in vivo* (Figure 3A). Corticosterone treatment increased phosphorylation of HTT at CDK5 sites, as indicated by immunoblotting of protein extracts from the whole cortex (Figures 3B and 3C) (* $p < 0.05$, Mann-Whitney test). CORT treatment also consistently increased the levels of CDK5 and p25 (** $p < 0.01$). We obtained similar though less marked results in protein extracts from the whole hippocampus.

Mice treated with CORT had lower levels of proBDNF and mature BDNF in cortical extracts than controls (** $p < 0.001$ and * $p < 0.05$, respectively) (Figure 3D). In the smaller hippocampal-only samples we could measure only mature BDNF: CORT-treated hippocampi had less mature BDNF than controls (**** $p < 0.0001$) (Figure 3E). Together with the fact that the transport assays are done with mCherry-BDNF expressed under a PGK promoter, ensuring that BDNF expression levels are the same between the different conditions, these data confirm that CORT reduces BDNF transport, not maturation. Chronic corticosterone treatment thus raises CDK5 and p25 protein levels, increases HTT phosphorylation at CDK5 sites, and reduces mature BDNF levels in the mouse cortex and hippocampus.

Phospho-ablation of HTT at CDK5 sites preserves neurogenesis under chronic CORT treatment

Since CORT reduces the number of newborn neurons and alters their morphology (Schoenfeld and Gould, 2013), we evaluated hippocampal neurogenesis in the dentate gyrus (DG) of WT and *Hdh*^{S1181A/S1201A} mice in control and CORT conditions (Figure 3A). We evaluated the dorsal and ventral regions of the DG separately, as they are thought to play different roles in cognitive and emotional processing. Because the results were similar in these two regions (Figure S2), however, we pooled the data (Figures 4A to 4C).

WT and *Hdh*^{S1181A/S1201A} mice had a similar basal rate of progenitor cell proliferation, according to the number of Ki67 cycling cells (Figures 4A and S2A). CORT treatment reduced proliferation in the WT DG (two-way ANOVA, ** $p < 0.01$) but had no effect on proliferation in *Hdh*^{S1181A/S1201A} mice (Figures 4A and S2A). To date the birth of the newborn cells, we injected BrdU at the beginning of CORT treatment and counted the surviving BrdU+ cells after four to six weeks of treatment (Figures 4B and S2B). These cells survived longer in *Hdh*^{S1181A/S1201A} mice than in WT mice (Two-way ANOVA, ** $p < 0.01$), and this effect was maintained under CORT treatment (Two-way ANOVA, ** $p < 0.01$).

To determine whether CORT affects the number of newly generated neurons in the DG, we used DCX, a transient marker of immature neurons. CORT did not affect the number of young neurons in either genotype (Figures 4C and S2C). The absence of an effect on newly generated neurons in conjunction with greater survival and proliferation led us to investigate whether neuronal maturation is accelerated in the mutant DG. Quantifying the number of BrdU+ cells that differentiated into mature neurons positive for calbindin, a terminal marker for granule neurons, revealed that *Hdh*^{S1181A/S1201A} mice showed greater neuronal differentiation than WT mice ($p < 0.05$) in the basal (vehicle) condition (Figures 4D and 4E). Chronic CORT treatment decreased terminal differentiation in WT mice ($p < 0.05$) but had no effect on *Hdh*^{S1181A/S1201A} mice.

We then measured the length and complexity of dendrites in WT and *Hdh*^{S1181A/S1201A} DCX+ neurons (Figures 4F to 4H). *Hdh*^{S1181A/S1201A} neurons have longer neurites and greater complexity than WT neurons under control conditions. CORT markedly shortened and simplified dendrites in WT mice compared to vehicle-treated control mice (Mendez-David et al., 2014). CORT also shortened and simplified

dendrites in *Hdh*^{S1181A/S1201A} mice compared to vehicle-treated *Hdh*^{S1181A/S1201A} mice, but the protective effect of unphosphorylatable HTT was still evident: the dendrites remained significantly longer and the neuritic complexity higher in CORT-treated *Hdh*^{S1181A/S1201A} mice than CORT-treated WT mice.

Preventing phosphorylation of HTT serines 1181 and 1201 in mice thus allows proliferation, survival and neuronal maturation to continue in the DG even in the presence of chronic CORT administration. We conclude that CORT-mediated effects require HTT phosphorylation at CDK5 sites.

Phospho-ablation of HTT at CDK5 sites decreases depression-related behaviors after chronic CORT treatment

We next examined whether HTT's phosphorylation status affects various stress-related behaviors in mice (Figure 5A). We first evaluated anxiety-like behaviors. In the open field test, vehicle-treated WT and *Hdh*^{S1181A/S1201A} mice spent the same amount of time in the center of the field. CORT treatment decreased the amount of time WT mice spent in the center (Two-way ANOVA, *** $p < 0.001$), as expected (David et al., 2009), and produced a similar effect in *Hdh*^{S1181A/S1201A} mice (Two-way ANOVA, ** $p < 0.01$) (Figure S3A). The total distance travelled was similar, so neither genotype nor treatment affected motor performance (Figure S3B). In the elevated plus maze test, vehicle-treated WT and *Hdh*^{S1181A/S1201A} mice spent a similar amount of time in the open arms (Figure S3C). CORT reduced the time both WT (* $p < 0.05$) and *Hdh*^{S1181A/S1201A} mice (** $p < 0.001$) spent in the open arms (Figure S3C). The total entries in open arms were similar for the two genotypes, confirming the absence of motor deficits (Figure S3D). Thus, phospho-ablation of HTT at CDK5 sites does not attenuate the anxiogenic effects of CORT.

To examine neurogenesis-dependent antidepressant effects of the mutation, we used the novelty suppressed feeding test (NSF), in which latency to feed indicates a depressed state (David et al., 2009; Santarelli et al., 2003). Mice were starved for 24h and then put in the presence of a food pellet situated at the center of a brightly lit open field. CORT treatment increased the latency to feed in both genotypes (WT vehicle vs CORT: Two-way ANOVA, **** $p < 0.0001$; *Hdh*^{S1181A/S1201A} vehicle vs CORT, Two-way

ANOVA, ** $p < 0.01$) but with lower efficacy in *Hdh*^{S1181A/S1201A} mice (WT CORT vs *Hdh*^{S1181A/S1201A} CORT, Two-way ANOVA, **** $p < 0.0001$) (Figure 5B).

Unphosphorylatable HTT thus protects against CORT treatment specifically in the NSF paradigm. Since the NSF paradigm is predictive of the behavioral outcome of antidepressants requiring increased hippocampal neurogenesis (David et al., 2009; Santarelli et al., 2003), our results suggest that the protective effect of phosphomutant HTT requires the maintenance of neurogenesis.

As a negative control, we tested a behavior that is associated with depressive states but is reported in most studies to be independent of neurogenesis: self-neglect (lack of grooming behavior) (Culig et al., 2017; Santarelli et al., 2003). We used the splash test (ST), in which a 10% sucrose solution is sprayed on the mouse snout to dirty the coat, and measured the duration of subsequent grooming over a 5-min period. WT and *Hdh*^{S1181A/S1201A} mice both spent less time grooming under CORT treatment (** $p < 0.001$ and * $p < 0.05$, respectively, Two-way ANOVA) (Figure 5C). Phospho-ablation does not appear to alter the depressive effects of CORT in this paradigm, which supports the notion that the behavioral differences we did observe between WT and *Hdh*^{S1181A/S1201A} mice are dependent on hippocampal neurogenesis.

To address this point more directly, we crossed *Hdh*^{S1181A/S1201A} mice with GFAP-thymidine kinase mice (Tk+) and specifically ablated neurogenesis in Tk+ mice by administering ganciclovir, as confirmed by evaluating cells positive for DCX (Figure 5D). All mice were treated with CORT and behavior was first tested in the NSF paradigm (Figure 5E). As before (Figure 5B), *Hdh*^{S1181A/S1201A} mice with preserved neurogenesis (Tk-) showed shorter latency to feed than WT (Tk-) mice (One-way ANOVA, **** $p < 0.001$), confirming the protective effect of the mutation against CORT treatment. Strikingly, ablation of neurogenesis in *Hdh*^{S1181A/S1201A} mice resulted in loss of their resistance to depression-like behavior (Tk- vs Tk+: One-way ANOVA, * $p < 0.05$). There was no difference between WT and *Hdh*^{S1181A/S1201A} mice with preserved (Tk-) or ablated (Tk+) neurogenesis in grooming duration in the ST (Figure 5F).

DISCUSSION

The molecular mechanisms by which chronic stress conditions reduce BDNF levels

in the hippocampus have been poorly understood. Our results dovetail nicely with previous studies showing that CDK5 is activated in several chronic stress paradigms in different brain regions, including the cortex, by increasing either CDK5 levels (Papadopoulou et al., 2015), the number of neurons expressing CDK5 (Bignante et al., 2010), cleavage of the p35 activator of CDK5 into its constitutive activated form p25 (Adzic et al., 2009; Bavley et al., 2017), or the localization of p35 at the cell membrane (Zhu et al., 2012). One study showed that CDK5 over-activation by p25 disrupts retrograde transport of various cargos, including signaling endosomes and mitochondria in dorsal root ganglion neurons (Klinman and Holzbaur, 2015); the authors found that hyper-activated CDK5 phosphorylates the nuclear distribution protein nudE-like 1 (Ndel1), which, in association with Lis1, increases attachment of the motor protein dynein to microtubules, diminishing organelle motility. Whether this mechanism is involved in the reduced transport of BDNF in response to CORT is unknown. If this is the case, it remains to be established whether and how the CDK5/HTT and CDK5/Ndel1/Lis1 pathways co-ordinate with each other.

Our data support the idea that precise regulation of the CDK5 pathway is required for neuronal homeostasis, as both downregulation and over-activation of CDK5 are detrimental. For instance, genetic inhibition of CDK5 impairs neurogenesis (Jessberger et al., 2008; Lagace et al., 2008), and restoration is beneficial (Lee et al., 2013). Very few studies have performed both molecular and behavioral studies, however. Zhu et al. reported that mild stress over a three-week period increases CDK5 activity (Zhu et al., 2012); the authors used a sucrose preference test to measure anhedonia. Although this report is consistent with our results, we should note that anhedonia is less associated with hippocampal neurogenesis than with impairment of the mesolimbic system (Russo and Nestler, 2013). Bignante et al. studied the rat amygdala in response to acute stress and found that increased CDK5/p35 activity correlated with poor performance in the elevated plus maze, while inhibiting CDK5 reversed these effects (Bignante et al., 2010). Conversely, non-stressed mice in which CDK5 is depleted in the dopaminergic neurons of the ventral tegmental area responded to the open field test with anxiety-like behavior and showed depressive behaviors in the sucrose preference and novelty suppressed feeding tests (Zhong et al., 2014).

It seems, then, that not only must CORT levels be tightly regulated, but that this regulation differs depending on the specific brain regions or neuronal groups involved. The unphosphorylatable HTT does not interfere with CORT-induced anxiety as assessed in the open field or the elevated plus maze, suggesting that the CDK5-HTT pathway may not affect the functions of the amygdala and the mesolimbic dopaminergic pathway (Corral-Frias et al., 2013; Tye et al., 2011). Instead, hyper-activation of the CDK5-HTT pathway provides resilience to CORT-induced depressive-like behavior in the novelty suppressed feeding assay, an effect that is lost when neurogenesis is ablated in GFAP-Tk+/Hdh^{S1181A/S1201A} mice. However, abolishing S1181/1201 phosphorylation did not confer complete resistance to stress in the NSF assay (Figure 5B). Also, the mutation did not completely restore decreased DCX neuronal maturation upon CORT treatment (Figures 4F to 4H). Sustained BDNF delivery from the cortical compartment may not fully compensate for the reduction of BDNF levels observed in stressed hippocampi.

Hyper-activated CDK5 may also modulate neurogenesis independently of HTT phosphorylation. For instance, CDK5 phosphorylates TrkB in dendrites of cortical neurons, which is necessary for proper BDNF-stimulated dendritic growth (Cheung et al., 2007). The glucocorticoid receptor is another target of CDK5, and phosphorylation of the nuclear glucocorticoid receptor alters its transcriptional activity (Adzic et al., 2009). Another example is the phosphorylation of the phosphodiesterase-4 by CDK5, which decreases cAMP signaling (Plattner et al., 2015): inhibiting this phosphorylation in the ventral striatum improves the performance of mice in the forced swim test (Plattner et al., 2015). Although these studies were performed in unstressed conditions, one can imagine that upon CORT treatment of Hdh^{S1181A/S1201A}, CDK5 may still target these pathways and affect anxiety/depressive-like behavior.

Over-activation of CDK5 is also involved in several pathways participating in the neurodegenerative processes in Alzheimer's disease, Parkinson's disease, and amyotrophic lateral sclerosis (Crews et al., 2011; Kawauchi, 2014; Park et al., 2019). Historically, HTT has been studied primarily in its polyglutamine-expanded form, which is responsible for Huntington's disease (HD). Strikingly, HD patients suffer from anxiety and depression up to 10 years before the onset of the motor symptoms of the disease

([Perlis et al., 2010](#)). In mouse models of HD, anxiety/depressive-like symptoms correlate with a reduction in hippocampal neurogenesis ([Pla P, 2014](#)), and in humans with HD, neurogenic activity is abnormally low ([Ernst et al., 2014](#)). We previously established that wild-type HTT contributes to several steps of adult hippocampal neurogenesis ([Ben M'barek et al., 2013](#); [Pla et al., 2013](#)). We now show that HTT also participates in the response to chronic stress, suggesting that at least part of the anxiety and depression evident in HD patients may be related to modification of the normal function of HTT. The relationship among HTT, CDK5, and BDNF represents a promising avenue for understanding the regulation of BDNF trafficking, hippocampal neurogenesis and affective mood.

AUTHOR CONTRIBUTIONS

F.A., D.J.D., F.S. and S.H. designed the study. F.A. and S.H. wrote the manuscript, which was commented on by all authors. F.A. performed most of the experiments. I.M.D. performed behavioral experiments and contributed to histology. W.C. performed all the microchambers experiments. R.C. contributed to western blotting and neuronal cultures. B.Y.B. contributed to mouse experiments and figures assembly.

ACKNOWLEDGMENTS

We kindly thank Caroline Benstaali, Béatrice Blot, Ayma Galland, Elodie Martin and staff of animal facilities (GIN and SFR-UMS Institut Paris Saclay Innovation Thérapeutique) for technical support; Florence Appaix, Jacques Brocard, Yasmina Saoudi of the GIN imaging facility platform (PIC-GIN) for help with image acquisitions; Vicky Brandt for helpful comments on the manuscript; Heather Cameron (NIMH/NIH) for supplying the GFAP-Tk mice (license agreement L-O 15-2015/0 between the National Institutes of Health and Université Paris-Sud). This work was supported by grants from Agence Nationale pour la Recherche (ANR-15-IDEX-02 NeuroCoG in the framework of the “Investissements d’avenir” program, S.H., F.S.; AXYON: ANR-18-CE16-0009-01, S.H., F.S.), Fondation pour la Recherche Médicale (FRM, équipes labellisées DEQ20170336752, S.H. and DEI20151234418, F.S.), Fondation pour la Recherche sur le Cerveau (FRC, S.H.), AGEMED program from INSERM (S.H., F.S.), ITMO Cancer Aviesan (Alliance Nationale Pour les Sciences de la Vie et de la Santé) in the context of the Plan cancer (slide scanner).

DECLARATION OF INTERESTS

The other authors declare no conflict of interest.

FIGURE LEGENDS

Figure 1. Corticosteroid treatment reduces cortico-hippocampal BDNF transport.

(A) Schematic of the three-compartment microfluidic device.

(B) Cortical axons (Tau positive) cross the axonal channels and contact hippocampal dendrites (MAP2 positive) in the synaptic chamber. Scale bar, 30 μm .

(C) Representative kymographs show BDNF vesicles trafficking in WT cortical axons treated or not (with DMSO) for 3h with dexamethasone (DXM). Graphs correspond to the corresponding kinetic analyses (at least 76 axons analyzed in 4 different cultures). Scale bar, 10 μm .

(D, E) Cortical neurons were treated (D) or transduced with viruses (E) as indicated and extracts were analyzed by immunoblotting for the presence of the phosphorylated forms of HTT at CDK5 sites (P-S1181 and P-S1201), HTT (D7F7), p35 and p25. Rosco: roscovitine. Histograms correspond to the quantitative evaluation of the indicated proteins (at least 5 independent cultures).

Error bars, SEM. * $p < 0.05$, ** $p < 0.01$. See also [Figure S1](#).

Figure 2. CDK5 mediates the decrease of cortico-hippocampal BDNF transport induced by corticosteroid through HTT phosphorylation at S1181/S1201

(A) Representative kymographs show BDNF vesicles trafficking in control and p25 expressing WT cortical axons. Graphs correspond to the corresponding kinetic analyses (at least 44 axons analyzed in 3 different cultures).

(B) Representative kymographs show BDNF vesicles trafficking in control and CDK5-KD expressing WT cortical axons treated or not (with DMSO) for 3h with dexamethasone (DXM). Graphs correspond to the corresponding kinetic analyses (at least 45 axons analyzed in 3 different cultures).

(C) Representative kymographs show BDNF vesicles trafficking in *Hdh*^{S1181A/S1201A} cortical axons treated or not (with DMSO) for 3h with dexamethasone (DXM). Graphs correspond to the corresponding kinetic analyses (at least 66 axons analyzed in 3 different cultures).

(D) Representative kymographs show BDNF vesicles trafficking in control and p25 expressing *Hdh*^{S1181A/S1201A} cortical axons. Graphs correspond to the corresponding kinetic analyses (at least 42 axons analyzed in 3 different cultures). Scale bars, 10 μ m. Error bars, SEM. *p<0.05. See also [Figure S1](#).

Figure 3. Huntingtin is phosphorylated at CDK5 sites upon chronic CORT treatment.

(A) WT mice were treated with CORT or Vehicle for 4 to 6 weeks in their drinking water. (B-E) Whole cortical and hippocampal (Hipp.) extracts were analyzed by immunoblotting for the presence of the phosphorylated forms of HTT at CDK5 sites (P-S1181 and P-S1201), total HTT (D7F7), CDK5, p35, p25, α -tubulin, pro and mature BDNF. Histograms correspond to the quantitative evaluation of the indicated proteins (at least 4 animals). Error bars, SEM. *p<0.05, **p<0.01, **** p<0.0001.

Figure 4. Phosphorylation of HTT at S1181/S1201 influences hippocampal neurogenesis.

(A-C) Cells counts were performed in the DG of Vehicle- and CORT-treated WT and *Hdh*^{S1181A/S1201A} mice (at least 4 for animals per condition) to quantify proliferation (Ki67+ cells, A), survival (BrdU+ cells, B) and immature neurons (DCX+ cells, C). *p<0.05, **p<0.01, ***p<0.001. (D) Representative images show BrdU+ surviving cells (cyan) expressing (or not) the terminal marker for granule cell differentiation calbindin (magenta) on DG sections of WT and *Hdh*^{S1181A/S1201A} mice treated with Vehicle or CORT. (E) The histogram shows the quantification of the number of BrdU+ and calbindin+ cells (3 animals per condition). *p<0.05, **p<0.01. (F, G) Dendritic length (F) and complexity (G) were evaluated in both genotypes and treatment conditions (3 animals per condition). (H) Representative drawings of dendrites of DCX-positive neurons. *p<0.05, **p<0.01, ***p<0.001, ****p<0.0001 comparing the *Hdh*^{S1181A/S1201A}-vehicle group with the WT vehicle group, \$p<0.05, \$\$p<0.01, \$\$\$p<0.001, \$\$\$\$p<0.0001 comparing the

Hdh^{S1181A/S1201A}-CORT group with the WT CORT group.

Error bars, SEM. See also [Figure S2](#).

Figure 5. Phosphoablation of HTT at CDK5 sites protects against corticosterone-induced suppression of hippocampal neurogenesis.

(A) WT and *Hdh*^{S1181A/S1201A} mice were treated for 4-6 weeks with CORT (A-C).

(B) Novelty suppressed feeding (NSF) test: latency to feed was expressed as percentage of animals that have not eaten over 10 minutes (left) and mean latency to feed (right) (11 to 27 mice per group).

(C) Splash test: grooming duration was measured after 10% sucrose solution was sprayed on the mouse coat (18 to 29 animals per group).

(D) Ganciclovir was administrated to WT and *Hdh*^{S1181A/S1201A} mice crossed with GFAP-Tk mice. All mice were treated with CORT (D-E). Middle and right: Cells counts were performed in *Hdh*^{S1181A/S1201A}/Tk⁻ and in *Hdh*^{S1181A/S1201A}/Tk⁺ treated with CORT to quantify DCX⁺ cells (4 animals per group).

(E) NSF was performed in neurogenesis-ablated (Tk⁺) and non-ablated (Tk⁻) mice (6 to 9 mice per group). Latency to feed was expressed as percentage of animals that have not eaten over 10 minutes (left) and mean latency to feed (right) (6 to 9 animals per group).

(F) Splash test: grooming duration was measured after 10% sucrose solution is sprayed on the mouse coat (6 to 9 animals per group).

Error bars, SEM. *p<0.05, **p<0.01, ***p<0.001, ****p<0.0001. See also [Figure S3](#).

STAR ★METHODS

RESOURCE AVAILABILITY

Lead contact

Further information and requests for resources and reagents should be directed to and will be fulfilled by the Lead Contact, Sandrine Humbert (sandrine.humbert@univ-grenoble-alpes.fr).

Materials availability

This study did not generate new unique reagents.

Data and Code Availability

This study did not generate/analyze datasets/code.

EXPERIMENTAL MODEL AND SUBJECT DETAILS

In vivo experiments were performed with 6- to 8-week-old male C57BL/6J mice, either wild-type (WT) or homozygous for the *Hdh*^{S1181A/S1201A} mutation ([Ben M'barek et al., 2013](#)), and all derived from heterozygous crosses.

Genetic suppression of hippocampal neurogenesis in WT and homozygous *Hdh*^{S1181A/S1201A} male mice was performed by crossing heterozygous *Hdh*^{S1181A/S1201A} male mice with GFAP-TK heterozygous female mice that express the herpes simplex virus (HSV) TK under the control of the glial fibrillary acidic protein (GFAP) promoter (GFAP-TK mice) ([Bush et al., 1998](#)). Mice were generated as previously described ([Mendez-David et al., 2017b](#)). An agreement (license L-O 15-2015/0) between the NIH and the Université Paris-Sud provides CESP/UMRS 1178 laboratory with the use of transgenic GFAP-TK mice ([Mendez-David et al., 2017b](#); [Snyder et al., 2011](#)), which were developed in the laboratory of Dr. Heather Cameron of the National Institute of Mental Health (NIMH).

All experimental procedures were performed in authorized establishments (Grenoble Institute of Neurosciences, INSERM U1216, license #B3851610008 and CEE26 authorization 2012-099 at Université Paris-Sud) in strict accordance with the

local animal welfare committee (Comité Local Grenoble Institute Neurosciences, C2EA-04), EU guidelines (directive 2010/63/EU) and the French National Committee (2010/63) for care and use of laboratory animals.

METHOD DETAILS

Primary neuronal culture in microfluidic devices

Whole cortices and hippocampi were dissected from E15.5 WT C57BL/6J or HdhS1181A/S1201A mice embryos and re-suspended in growing medium (Neurobasal medium supplemented with 2% B27, 2 mM Glutamax, and 1% penicillin/streptomycin). We established cortico-hippocampal neuronal networks in microfluidic devices (Virlogeux et al., 2018) coated overnight at 4°C with poly-D-lysine (0.1 mg/ml) in the upper and synaptic chambers, and with a mix of poly-D-lysine (0.1 mg/ml) and laminin (10 µg/ml) in the lower chamber. This generated a gradient of laminin reducing the number of hippocampal axons reaching the synaptic chamber (Virlogeux et al., 2018). Microchambers were washed 3 times with growing medium and placed at 37°C before neurons were plated.

First, cortical neurons were plated in the presynaptic compartment so that they can extend axons through the 500 µm-long microgrooves to the synaptic compartment. Then, hippocampal cells were seeded into the postsynaptic compartment and extended dendrites through 75 µm-long microgrooves to the synaptic compartment. Cells were plated at a density of approximately 7000 cells/mm² in the microfluidic devices (Virlogeux et al., 2018). The day after plating, neurons were infected for 48h with the following lentiviruses (LV): LV.PGK.BDNF-mCh, LV.EF1α-GFP, LV.EF1α.p25-GFP (derived from plasmid #1343, Addgene) and LV.EF1α.CDK5-KD-GFP (derived from plasmid #1344, Addgene). The equivalent of 1x10⁷ genomic particles were used to transfect the neurons in their respective chambers and culture dishes. Transduction efficiency has been determined in three different cultures. At DIV7, cortical neurons were fixed in 4% paraformaldehyde, rinsed in PBS, permeabilized in 0.1% Triton and incubated overnight at 4°C with anti-GFP (1/200, Abcam, ab13970). Preparations were rinsed, incubated with Alexa Fluor® 488 goat anti-chicken (1/500, ThermoFisher,

A11039) and Hoechst33342 (2µg/ml, ThermoFisher, H3570) to counterstain nuclei, and mounted in Dako mounted medium (Agilent, S302380-2). Confocal images were acquired using an inverted confocal microscopy (LSM710, Zeiss) and analyzed using ImageJ (<https://imagej.nih.gov/ij/download.html>). Quantification is provided in Supplemental [Figure S1](#).

Live-cell and confocal imaging

Live-cell recordings were acquired using an inverted microscope (Axio Observer, Zeiss) coupled to a spinning-disk confocal system (CSU-W1-T3, Yokogawa) connected to a wide field electron-multiplying CCD camera (ProEM+1024, Princeton Instrument) and maintained at 37°C and 5% CO₂. Images were taken every 200 ms for 30 s to study BDNF-mCh trafficking (×63 oil-immersion objective, 1.46 NA).

Kymograph analysis

Kymographs were generated using KymoToolBox plugin for ImageJ with a length of 100 µm (x-axis) and a total time of 30 s (y-axis). Anterograde and retrograde velocities, vesicle numbers and net flux were analyzed as previously described ([Virlogeux et al., 2018](#); [Zala et al., 2013](#)). Only vesicles with a velocity above 0.12 µm/s were considered motile. For each condition, at least six chambers from three independent cultures were used and a minimum of 40 axons was analyzed.

CORT treatment to mimic stress and behavioral testing

Mice, either wild-type (WT) or homozygous for the *Hdh*^{S1181A/S1201A} mutation, were treated for four to six weeks with a vehicle (0.45 % hydroxypropyl-β-cyclodextrin, Roquette, Cat#965440) or with CORT (35 µg/ml/day, dissolved in vehicle) added to their drinking water. Mice were injected with 150 mg/kg of BrdU twice per day for 3 days before the CORT treatment session ([Figure 2A](#)).

Genetic suppression of hippocampal neurogenesis in WT and homozygote *Hdh*^{S1181A/S1201A} male mice was performed by crossing heterozygous *Hdh*^{S1181A/S1201A} male mice with GFAP-Tk heterozygous female mice that express the herpes simplex virus (HSV) Tk under the control of the glial fibrillary acidic protein (GFAP) promoter

(GFAP-Tk mice) ([Bush et al., 1998](#)). Male mice from the four genotypes (up to six months old) were given ValGanciclovir (VGCV, Roche), the L-valyl ester of ganciclovir, from Monday to Friday for eight weeks, through their chow, at a concentration of 15 mg/kg/day to kill mitotically active cells. Mice received CORT as previously described during the last four weeks of VGCV feeding.

We evaluated anxiety- and depression-like behavior in mice using the open field (OF), elevated plus maze (EPM), sucrose splash test (ST), and novelty suppressed feeding (NSF) tests as described previously ([David et al., 2009](#); [Mendez-David et al., 2017a](#); [Mendez-David et al., 2014](#); [Mendez-David et al., 2017b](#)). Behavioral tests were conducted between 8:00 am and 12:00 pm.

Western Blot

Cortical neurons in culture were treated for 3h with DXM (5 μ M), the selective inhibitor of CDK5 roscovitine (10 μ M) or both drugs and harvested in protein extraction buffer (Tris-HCl 20 mM, pH7.4, NaCl 137mM, EDTA 2mM, Triton X-100 1%, supplemented with 1/100 protease and phosphatases inhibitors (Sigma-Aldrich, P8340 and P5726) and frozen at -80°C until protein extraction. Brain samples (whole cortices and hippocampi) were obtained from mice sacrificed by quick cervical dislocation and dissection under a stereomicroscope. Brain tissues were frozen at -80°C until protein extraction. Protein extraction of neurons was performed by pipetting up and down approximately 10 times with a P1000 Gilson. Cortices and hippocampi were dissociated using 10 strokes of the pestle of a tight-fitting Dounce homogenizer. The supernatants of both samples were collected after centrifugation at 10,000 rpm for 10 min at 4°C. Protein concentration was measured by the BCA method. Proteins (20 μ g total) were treated with SDS-PAGE sample buffer [6X concentrated: 350 mM Tris, 10% (w/v) SDS, 30% (v/v) glycerol, 0.6 M DTT, 0.06% (w/v) bromophenol blue], boiled 5 min at 95°C, and loaded on 15% (for CDK5, p35, p25 and BDNF detection) and 6% (for HTT) acrylamide/bisacrylamide gels. Proteins were transferred onto PVDF (polyvinylidene difluoride) membranes, blocked with 5% bovine serum albumin and 0.5% Tween (Euromedex) in TBS (TBST) for 1h at room temperature, and probed overnight at 4°C with the following primary antibodies diluted in 5% bovine serum albumin-TBST: 1:200

rabbit anti-CDK5 (C8, sc-173) antibody, 1:200 mouse anti-CDK5 (J3, sc-6247) antibody, 1:200 rabbit anti-p35/p25 (C19, sc-820) antibody, 1:500 rabbit anti-BDNF (N20, sc-546) antibody (all from Santa Cruz Biotechnology), 1:1000 rabbit anti-BDNF (ab108319) antibody (Abcam), 1:1000 rabbit anti-huntingtin (D7F7, #5656) antibody (Cell Signalling Technologies) and 1:5000 mouse anti-alpha tubulin (T9026, Sigma-Aldrich). HTT-specific antibodies against phospho-serine 1181 and phospho-serine 1201 were generated following immunization of rabbits with synthesized sequences PSLTNPPSL[pS]PIR (1181) and PGEQASTPM[Sp]PKKV (1201) (Covalab, Lyon, France) and were used at 1:100 in 5% bovine serum albumin-TBST for western blot. They were validated by immunoblotting of cytoplasmic and nuclei-derived protein fractions obtained from WT and *Hdh*^{S1181A/S1201A} mouse embryonic fibroblasts (Figure S1B). Membranes were washed with TBST, incubated for 1h at room temperature with horseradish peroxidase-conjugated secondary antibodies (1:5000 goat anti-rabbit IgG (H+L), from Jackson ImmunoResearch; 1:5000 goat anti-mouse IgG1, SouthernBiotech), and visualized using Pico and ECL western blotting substrate (ThermoFisher Scientific) on a Chemidoc imaging system (Biorad).

Histology and immunolabeling

Mice were sacrificed between 9:00 am and 3:00 pm. Mice were anesthetized with ketamine (250 mg/ml; 100 μ l/10 g of body weight, intraperitoneal injections) and intracardiacally perfused with PBS followed by cold paraformaldehyde (PFA) 4%. Brains were harvested, post-fixed for 2h in PFA 4%, cryopreserved in 30% sucrose and embedded in OCT Compound (VWR International). Brains were cryosectioned (35 μ m) through the entire hippocampus and slices were kept in free-floating at -20°C in anti-freeze solution (18.75% (w/v) sucrose, 37.5% (v/v) ethylene glycol, 0.05% (w/v) sodium azide in PBS). Proliferation and survival were assessed following immunolabeling of Ki67 (anti-Ki67 antibody: M3062, Spring Biosciences) and BrdU (anti-BrdU antibody: #347580, BD Biosciences) positive nuclei. Immature neurons expressing doublecortin (DCX, anti-DCX antibody: sc-8066, Santa Cruz Biotechnology) were immunostained. All staining protocols were already described in previous studies (David et al., 2009; Guilloux et al., 2017; Mendez-David et al., 2017b).

The maturation of newly generated neurons in the DG was examined by staining brain slices of WT and *Hdh*^{S1181A/S1201A} mice to reveal BrdU and calbindin positive neurons. Briefly, brain slices were mounted onto Superfrost Plus GOLD glass slides (Thermo Scientific, K5800AMNZ72), let to dry and adhere overnight, and then rehydrated for 5 min in PBS. Antigen retrieval was achieved by incubating the slices for 10 min at 95°C in citrate buffer pH 6 (1:10 in ultra-pure water, Zytomed Systems). Following 3 rinses in PBS, membranes were digested for 7 minutes in 0.1 % trypsin (diluted in 0.1 M Tris pH 7.2 with 0.1% CaCl₂), rinses and histones removal was achieved by incubating the slices for 30 min in 2N HCl. Slices were rinsed and blocked in 3% normal donkey serum in PBS containing 0.3% Triton-X100 for 1h at room temperature then incubated overnight at room temperature in 1:100 of mouse anti-BrdU antibody (#347580, BD Biosciences) and 1:500 rabbit anti-calbindin antibody (#13176, Cell Signaling Technologies). Slices were rinsed, incubated in 1:500 647 donkey anti-rabbit antibody (A31573, ThermoFisher) and 1:250 cy2 donkey anti-mouse antibody (#715-225-150, Jackson ImmunoResearch) and Hoechst 33342 (2ug/ml) in PBS for 1h. After 3 rinses in PBS, slices were mounted in Dako mounting medium. Quantifications were performed on 1/6 of the hippocampus for BrdU+ cells; 1/12 for Ki67+ and DCX+ cells and 1/12 for calbindin/BrdU+ cells.

Immunocytochemistry

The proportion of neurons expressing reelin was evaluated in E15.5 whole cortex cultures from WT embryos. Neurons were fixed at 7DIV in 4% paraformaldehyde, rinsed in PBS, permeabilized in 0.1% Triton and incubated overnight at 4°C with goat anti-reelin (1/500, AF3820, R&D Systems) and mouse anti-βIII tubulin coupled to Cy3 (1/200, C4585, Sigma-Aldrich). After 1h incubation with Alexa Fluor® 488 donkey anti-goat (1/500, ThermoFisher, A11055) and Hoechst33342 (2μg/ml), preparations were rinsed and mounted in Dako mounted medium. The proportion of reelin expressing neurons was evaluated in 2 different cultures, in 2 different wells of culture within each experiment. Images were acquired on the Axio Scan.Z1 slide scanner (Colibri.7; 20X objective; Zeiss) and analyzed using the Zen software (<https://www.zeiss.com/microscopy/int/products/microscope-software/zen-lite.html>).

Quantification is provided in Supplemental [Figure S1](#).

Sholl analysis

Dendritic complexity and ramification length were assessed using the NeuroLucida software as described previously ([Guilloux et al., 2017](#); [Mendez-David et al., 2014](#); [Mendez-David et al., 2017b](#)).

QUANTIFICATION AND STATISTICAL ANALYSIS

For western blots, densitometry analyses of Pico and ECL signals were performed using NIH Image J software. Data are represented as mean \pm SEM of at least 4 animals per condition. Protein levels are displayed as percentage standardized to α tubulin, p35 and HTT. Statistical significance was assessed using a Mann-Whitney test. In histology experiments, cell counts from at least 4 animals per group were expressed as mean \pm SEM values. Statistical comparisons were made using the two-way ANOVA followed by the Tukey's multiple comparison *post hoc* tests. For the NSF test, a Kaplan–Meier survival analysis was applied in which the Mantel-Cox logrank test was used to evaluate differences between experimental groups. Animals that did not eat during the 10 min test period were attributed the value of 600 sec. In the NSF applied on GFAP-tk mice, statistical comparisons were made using the one-way ANOVA followed by the Tukey's multiple comparison *post hoc* tests. Statistical significance was set to $p < 0.05$. All analyses were conducted using Graph pad Prism 7.0. Statistical details of experiments are indicated in the figure legends. Complete statistical analyses related to figures 1 to 5 and to supplemental figures S1 to S3 are listed in [Supplemental Excel tables S1](#) and [S2](#) respectively.

REFERENCES

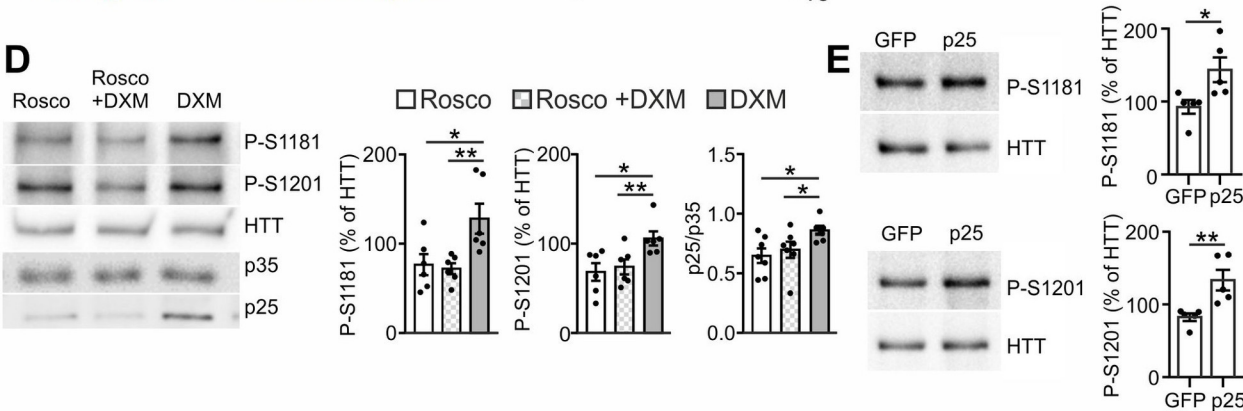
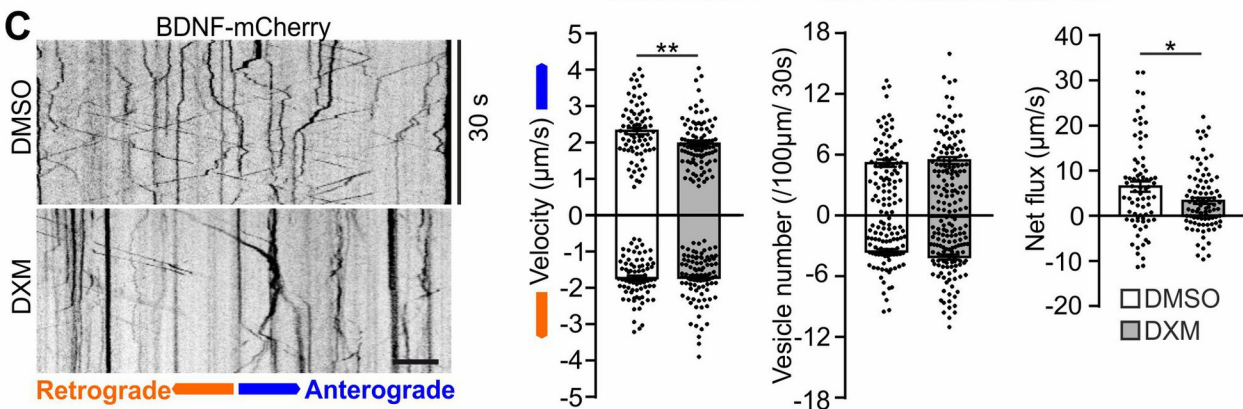
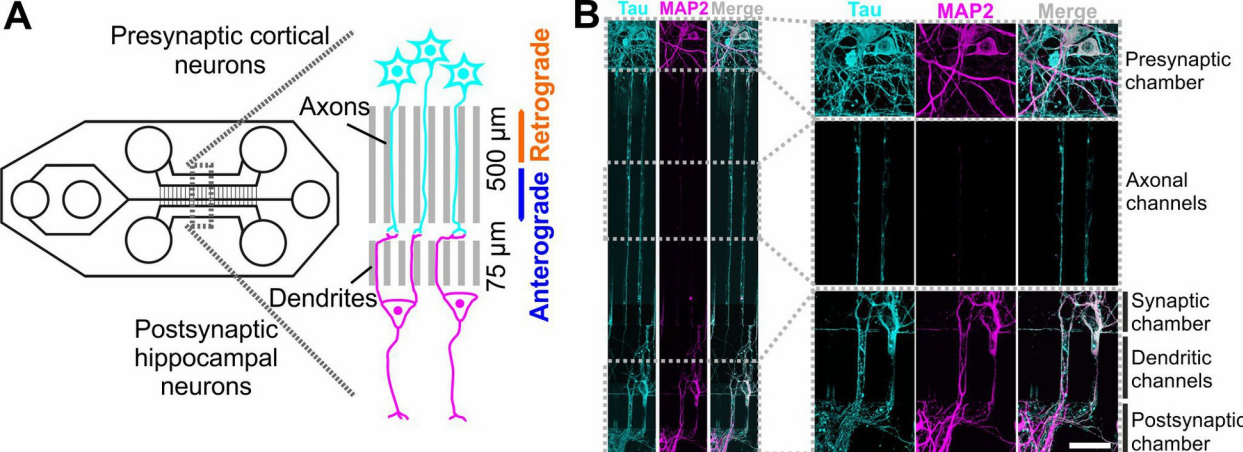
- Adzic, M., Djordjevic, J., Djordjevic, A., Niciforovic, A., Demonacos, C., Radojicic, M., and Krstic-Demonacos, M. (2009). Acute or chronic stress induce cell compartment-specific phosphorylation of glucocorticoid receptor and alter its transcriptional activity in Wistar rat brain. *J Endocrinol* 202, 87-97.
- Anacker, C., Luna, V.M., Stevens, G.S., Millette, A., Shores, R., Jimenez, J.C., Chen, B., and Hen, R. (2018). Hippocampal neurogenesis confers stress resilience by inhibiting the ventral dentate gyrus. *Nature* 559, 98-102.
- Bavley, C.C., Fischer, D.K., Rizzo, B.K., and Rajadhyaksha, A.M. (2017). Cav1.2 channels mediate persistent chronic stress-induced behavioral deficits that are associated with prefrontal cortex activation of the p25/Cdk5-glucocorticoid receptor pathway. *Neurobiol Stress* 7, 27-37.
- Ben M'barek, K., Pla, P., Orvoen, S., Benstaali, C., Godin, J.D., Gardier, A.M., Saudou, F., David, D.J., and Humbert, S. (2013). Huntingtin mediates anxiety/depression-related behaviors and hippocampal neurogenesis. *J Neurosci* 33, 8608-8620.
- Bignante, E.A., Paglini, G., and Molina, V.A. (2010). Previous stress exposure enhances both anxiety-like behaviour and p35 levels in the basolateral amygdala complex: modulation by midazolam. *Neuropsychopharmacology* 20, 388-397.
- Boldrini, M., Hen, R., Underwood, M.D., Rosoklija, G.B., Dwork, A.J., Mann, J.J., and Arango, V. (2012). Hippocampal angiogenesis and progenitor cell proliferation are increased with antidepressant use in major depression. *Biological psychiatry* 72, 562-571.
- Boldrini, M., Underwood, M.D., Hen, R., Rosoklija, G.B., Dwork, A.J., John Mann, J., and Arango, V. (2009). Antidepressants increase neural progenitor cells in the human hippocampus. *Neuropsychopharmacology* 34, 2376-2389.
- Bremner, J.D., Narayan, M., Anderson, E.R., Staib, L.H., Miller, H.L., and Charney, D.S. (2000). Hippocampal volume reduction in major depression. *Am J Psychiatry* 157, 115-118.
- Bruel-Jungerman, E., Davis, S., Rampon, C., and Laroche, S. (2006). Long-term potentiation enhances neurogenesis in the adult dentate gyrus. *J Neurosci* 26, 5888-5893.
- Bush, T.G., Savidge, T.C., Freeman, T.C., Cox, H.J., Campbell, E.A., Mucke, L., Johnson, M.H., and Sofroniew, M.V. (1998). Fulminant jejuno-ileitis following ablation of enteric glia in adult transgenic mice. *Cell* 93, 189-201.
- Chan, J.P., Cordeira, J., Calderon, G.A., Iyer, L.K., and Rios, M. (2008). Depletion of central BDNF in mice impedes terminal differentiation of new granule neurons in the adult hippocampus. *Mol Cell Neurosci* 39, 372-383.
- Chen, B., Dowlatshahi, D., MacQueen, G.M., Wang, J.F., and Young, L.T. (2001). Increased hippocampal BDNF immunoreactivity in subjects treated with antidepressant medication. *Biological psychiatry* 50, 260-265.
- Cheung, Z.H., Chin, W.H., Chen, Y., Ng, Y.P., and Ip, N.Y. (2007). Cdk5 is involved in BDNF-stimulated dendritic growth in hippocampal neurons. *PLoS Biol* 5, e63.

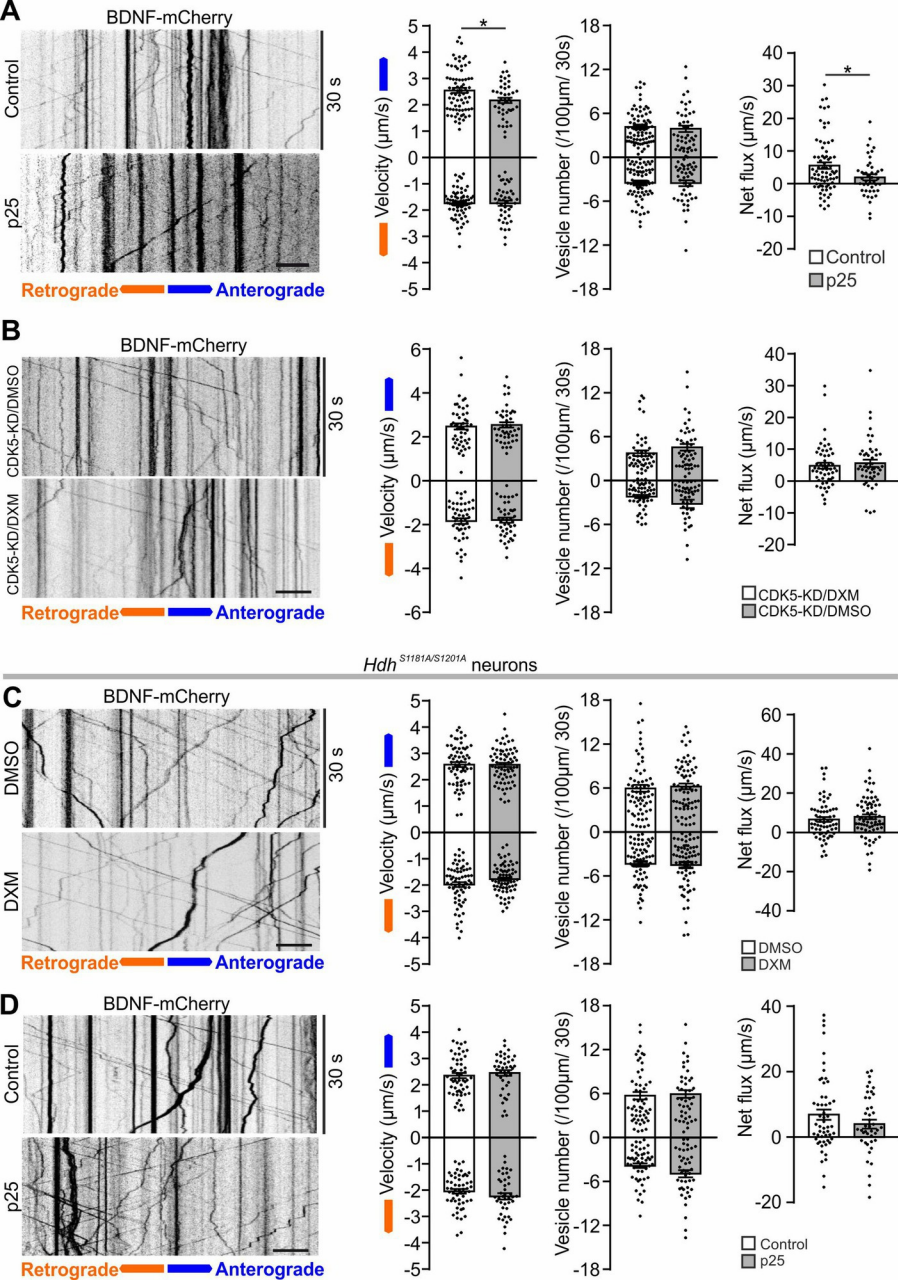
- Corral-Frias, N.S., Lahood, R.P., Edelman-Vogelsang, K.E., French, E.D., and Fellous, J.M. (2013). Involvement of the ventral tegmental area in a rodent model of post-traumatic stress disorder. *Neuropsychopharmacology* 38, 350-363.
- Crews, L., Patrick, C., Adame, A., Rockenstein, E., and Masliah, E. (2011). Modulation of aberrant CDK5 signaling rescues impaired neurogenesis in models of Alzheimer's disease. *Cell Death Dis* 2, e120.
- Culig, L., Surget, A., Bourdey, M., Khemissi, W., Le Guisquet, A.M., Vogel, E., Sahay, A., Hen, R., and Belzung, C. (2017). Increasing adult hippocampal neurogenesis in mice after exposure to unpredictable chronic mild stress may counteract some of the effects of stress. *Neuropharmacology* 126, 179-189.
- David, D.J., Samuels, B.A., Rainer, Q., Wang, J.W., Marsteller, D., Mendez, I., Drew, M., Craig, D.A., Guiard, B.P., Guilloux, J.P., Artymyshyn, R.P., Gardier, A.M., Gerald, C., Antonijevic, I.A., Leonardo, E.D., and Hen, R. (2009). Neurogenesis-dependent and -independent effects of fluoxetine in an animal model of anxiety/depression. *Neuron* 62, 479-493.
- Ernst, A., Alkass, K., Bernard, S., Salehpour, M., Perl, S., Tisdale, J., Possnert, G., Druid, H., and Frisen, J. (2014). Neurogenesis in the striatum of the adult human brain. *Cell* 156, 1072-1083.
- Gauthier, L.R., Charrin, B.C., Borrell-Pages, M., Dompierre, J.P., Rangone, H., Cordelieres, F.P., De Mey, J., MacDonald, M.E., Lessmann, V., Humbert, S., and Saudou, F. (2004). Huntingtin controls neurotrophic support and survival of neurons by enhancing BDNF vesicular transport along microtubules. *Cell* 118, 127-138.
- Guilloux, J.P., Samuels, B.A., Mendez-David, I., Hu, A., Levinstein, M., Faye, C., Mekiri, M., Mocaer, E., Gardier, A.M., Hen, R., Sors, A., and David, D.J. (2017). S 38093, a histamine H3 antagonist/inverse agonist, promotes hippocampal neurogenesis and improves context discrimination task in aged mice. *Sci Rep* 7, 42946.
- Hinckelmann, M.V., Virlogeux, A., Niehage, C., Poujol, C., Choquet, D., Hoflack, B., Zala, D., and Saudou, F. (2016). Self-propelling vesicles define glycolysis as the minimal energy machinery for neuronal transport. *Nat Commun* 7, 13233.
- Hirokawa, N., Niwa, S., and Tanaka, Y. (2010). Molecular motors in neurons: transport mechanisms and roles in brain function, development, and disease. *Neuron* 68, 610-638.
- Huang, T.L., Lee, C.T., and Liu, Y.L. (2008). Serum brain-derived neurotrophic factor levels in patients with major depression: effects of antidepressants. *J Psychiatr Res* 42, 521-525.
- Jessberger, S., Aigner, S., Clemenson, G.D., Jr., Toni, N., Lie, D.C., Karalay, O., Overall, R., Kempermann, G., and Gage, F.H. (2008). Cdk5 regulates accurate maturation of newborn granule cells in the adult hippocampus. *PLoS Biol* 6, e272.
- Kang, H., and Schuman, E.M. (1995). Long-lasting neurotrophin-induced enhancement of synaptic transmission in the adult hippocampus. *Science* 267, 1658-1662.
- Kawauchi, T. (2014). Cdk5 regulates multiple cellular events in neural development, function and disease. *Dev Growth Differ* 56, 335-348.

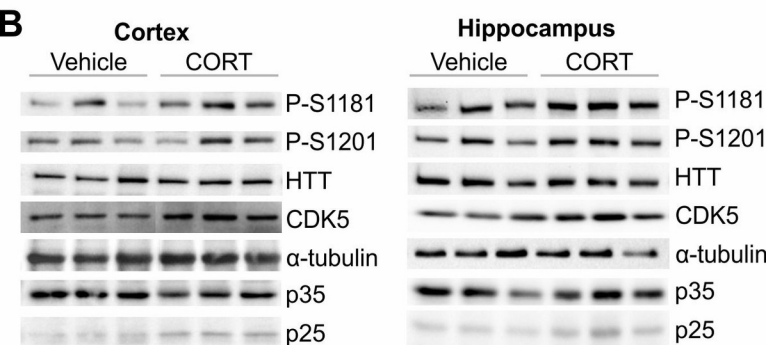
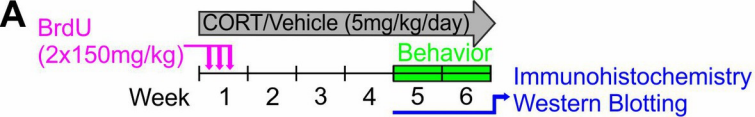
- Kempermann, G., Gage, F.H., Aigner, L., Song, H., Curtis, M.A., Thuret, S., Kuhn, H.G., Jessberger, S., Frankland, P.W., Cameron, H.A., Gould, E., Hen, R., Abrous, D.N., Toni, N., Schinder, A.F., Zhao, X., Lucassen, P.J., and Frisen, J. (2018). Human Adult Neurogenesis: Evidence and Remaining Questions. *Cell stem cell* *23*, 25-30.
- Klinman, E., and Holzbaur, E.L. (2015). Stress-Induced CDK5 Activation Disrupts Axonal Transport via Lis1/Ndel1/Dynein. *Cell Rep* *12*, 462-473.
- Lagace, D.C., Benavides, D.R., Kansy, J.W., Mapelli, M., Greengard, P., Bibb, J.A., and Eisch, A.J. (2008). Cdk5 is essential for adult hippocampal neurogenesis. *Proc Natl Acad Sci U S A* *105*, 18567-18571.
- Lee, M.H., Amin, N.D., Venkatesan, A., Wang, T., Tyagi, R., Pant, H.C., and Nath, A. (2013). Impaired neurogenesis and neurite outgrowth in an HIV-gp120 transgenic model is reversed by exercise via BDNF production and Cdk5 regulation. *J Neurovirol* *19*, 418-431.
- Mendez-David, I., Boursier, C., Domergue, V., Colle, R., Falissard, B., Corruble, E., Gardier, A.M., Guilloux, J.P., and David, D.J. (2017a). Differential Peripheral Proteomic Biosignature of Fluoxetine Response in a Mouse Model of Anxiety/Depression. *Frontiers in cellular neuroscience* *11*, 237.
- Mendez-David, I., David, D.J., Darcet, F., Wu, M.V., Kerdine-Romer, S., Gardier, A.M., and Hen, R. (2014). Rapid anxiolytic effects of a 5-HT(4) receptor agonist are mediated by a neurogenesis-independent mechanism. *Neuropsychopharmacology* *39*, 1366-1378.
- Mendez-David, I., Guilloux, J.P., Papp, M., Tritschler, L., Mocaer, E., Gardier, A.M., Bretin, S., and David, D.J. (2017b). S 47445 Produces Antidepressant- and Anxiolytic-Like Effects through Neurogenesis Dependent and Independent Mechanisms. *Frontiers in pharmacology* *8*, 462.
- Papadopoulou, A., Siamatras, T., Delgado-Morales, R., Amin, N.D., Shukla, V., Zheng, Y.L., Pant, H.C., Almeida, O.F., and Kino, T. (2015). Acute and chronic stress differentially regulate cyclin-dependent kinase 5 in mouse brain: implications to glucocorticoid actions and major depression. *Transl Psychiatry* *5*, e578.
- Park, J., Seo, J., Won, J., Yeo, H.G., Ahn, Y.J., Kim, K., Jin, Y.B., Koo, B.S., Lim, K.S., Jeong, K.J., Kang, P., Lee, H.Y., Baek, S.H., Jeon, C.Y., Hong, J.J., Huh, J.W., Kim, Y.H., Park, S.J., Kim, S.U., Lee, D.S., Lee, S.R., and Lee, Y. (2019). Abnormal Mitochondria in a Non-human Primate Model of MPTP-induced Parkinson's Disease: Drp1 and CDK5/p25 Signaling. *Exp Neurobiol* *28*, 414-424.
- Perlis, R.H., Smoller, J.W., Mysore, J., Sun, M., Gillis, T., Purcell, S., Rietschel, M., Nothen, M.M., Witt, S., Maier, W., Iosifescu, D.V., Sullivan, P., Rush, A.J., Fava, M., Breiter, H., Macdonald, M., and Gusella, J. (2010). Prevalence of incompletely penetrant Huntington's disease alleles among individuals with major depressive disorder. *Am J Psychiatry* *167*, 574-579.
- Pla, P., Orvoen, S., Benstaali, C., Dodier, S., Gardier, A.M., David, D.J., Humbert, S., and Saudou, F. (2013). Huntingtin acts non cell-autonomously on hippocampal neurogenesis and controls anxiety-related behaviors in adult mouse. *PLoS One* *8*, e73902.

- Pla P, O.S., Saudou F, David DJ and S Humbert (2014). Mood disorders in Huntington's disease : from behavior to cellular and molecular mechanisms. *Frontiers in behavioral neuroscience* 8, 1-15.
- Plattner, F., Hayashi, K., Hernandez, A., Benavides, D.R., Tassin, T.C., Tan, C., Day, J., Fina, M.W., Yuen, E.Y., Yan, Z., Goldberg, M.S., Nairn, A.C., Greengard, P., Nestler, E.J., Taussig, R., Nishi, A., Houslay, M.D., and Bibb, J.A. (2015). The role of ventral striatal cAMP signaling in stress-induced behaviors. *Nature neuroscience* 18, 1094-1100.
- Russo, S.J., and Nestler, E.J. (2013). The brain reward circuitry in mood disorders. *Nat Rev Neurosci* 14, 609-625.
- Santarelli, L., Saxe, M., Gross, C., Surget, A., Battaglia, F., Dulawa, S., Weisstaub, N., Lee, J., Duman, R., Arancio, O., Belzung, C., and Hen, R. (2003). Requirement of hippocampal neurogenesis for the behavioral effects of antidepressants. *Science* 301, 805-809.
- Saudou, F., and Humbert, S. (2016). The Biology of Huntingtin. *Neuron* 89, 910-926.
- Schoenfeld, T.J., and Gould, E. (2013). Differential effects of stress and glucocorticoids on adult neurogenesis. *Curr Top Behav Neurosci* 15, 139-164.
- Schoenfeld, T.J., McCausland, H.C., Morris, H.D., Padmanaban, V., and Cameron, H.A. (2017). Stress and Loss of Adult Neurogenesis Differentially Reduce Hippocampal Volume. *Biological psychiatry* 82, 914-923.
- Snyder, J.S., Soumier, A., Brewer, M., Pickel, J., and Cameron, H.A. (2011). Adult hippocampal neurogenesis buffers stress responses and depressive behaviour. *Nature* 476, 458-461.
- Stone, S.S., Teixeira, C.M., Devito, L.M., Zaslavsky, K., Josselyn, S.A., Lozano, A.M., and Frankland, P.W. (2011). Stimulation of entorhinal cortex promotes adult neurogenesis and facilitates spatial memory. *J Neurosci* 31, 13469-13484.
- Tye, K.M., Prakash, R., Kim, S.Y., Fenno, L.E., Grosenick, L., Zarabi, H., Thompson, K.R., Gradinaru, V., Ramakrishnan, C., and Deisseroth, K. (2011). Amygdala circuitry mediating reversible and bidirectional control of anxiety. *Nature* 471, 358-362.
- Virlogeux, A., Moutaux, E., Christaller, W., Genoux, A., Bruyere, J., Fino, E., Charlot, B., Cazorla, M., and Saudou, F. (2018). Reconstituting Corticostriatal Network on-a-Chip Reveals the Contribution of the Presynaptic Compartment to Huntington's Disease. *Cell Rep* 22, 110-122.
- Vyas, S., Rodrigues, A.J., Silva, J.M., Tronche, F., Almeida, O.F., Sousa, N., and Sotiropoulos, I. (2016). Chronic Stress and Glucocorticoids: From Neuronal Plasticity to Neurodegeneration. *Neural Plast* 2016, 6391686.
- Wang, L., Chang, X., She, L., Xu, D., Huang, W., and Poo, M.M. (2015). Autocrine action of BDNF on dendrite development of adult-born hippocampal neurons. *J Neurosci* 35, 8384-8393.
- Waterhouse, E.G., An, J.J., Orefice, L.L., Baydyuk, M., Liao, G.Y., Zheng, K., Lu, B., and Xu, B. (2012). BDNF promotes differentiation and maturation of adult-born neurons through GABAergic transmission. *J Neurosci* 32, 14318-14330.

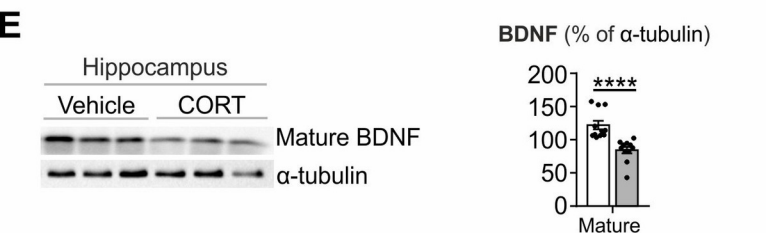
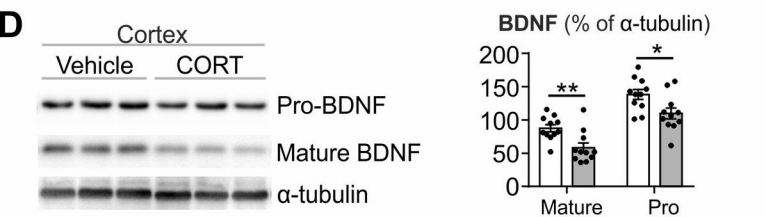
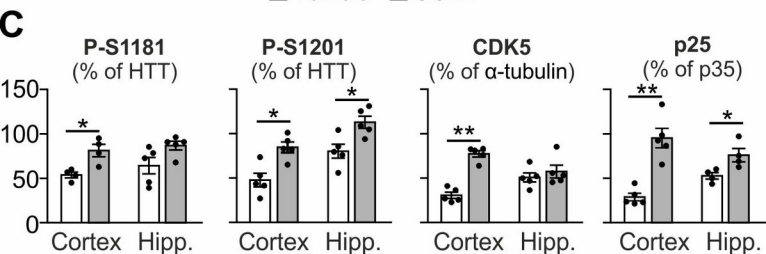
- Witter, M.P., Doan, T.P., Jacobsen, B., Nilssen, E.S., and Ohara, S. (2017). Architecture of the Entorhinal Cortex A Review of Entorhinal Anatomy in Rodents with Some Comparative Notes. *Front Syst Neurosci* 11, 46.
- Yun, S., Reynolds, R.P., Petrof, I., White, A., Rivera, P.D., Segev, A., Gibson, A.D., Suarez, M., DeSalle, M.J., Ito, N., Mukherjee, S., Richardson, D.R., Kang, C.E., Ahrens-Nicklas, R.C., Soler, I., Chetkovich, D.M., Kourrich, S., Coulter, D.A., and Eisch, A.J. (2018). Stimulation of entorhinal cortex-dentate gyrus circuitry is antidepressive. *Nat Med* 24, 658-666.
- Zala, D., Hinckelmann, M.V., Yu, H., Lyra da Cunha, M.M., Liot, G., Cordelieres, F.P., Marco, S., and Saudou, F. (2013). Vesicular glycolysis provides on-board energy for fast axonal transport. *Cell* 152, 479-491.
- Zhong, P., Liu, X., Zhang, Z., Hu, Y., Liu, S.J., Lezama-Ruiz, M., Joksimovic, M., and Liu, Q.S. (2014). Cyclin-dependent kinase 5 in the ventral tegmental area regulates depression-related behaviors. *J Neurosci* 34, 6352-6366.
- Zhu, W.L., Shi, H.S., Wang, S.J., Xu, C.M., Jiang, W.G., Wang, X., Wu, P., Li, Q.Q., Ding, Z.B., and Lu, L. (2012). Increased Cdk5/p35 activity in the dentate gyrus mediates depressive-like behaviour in rats. *Int J Neuropsychopharmacol* 15, 795-809.

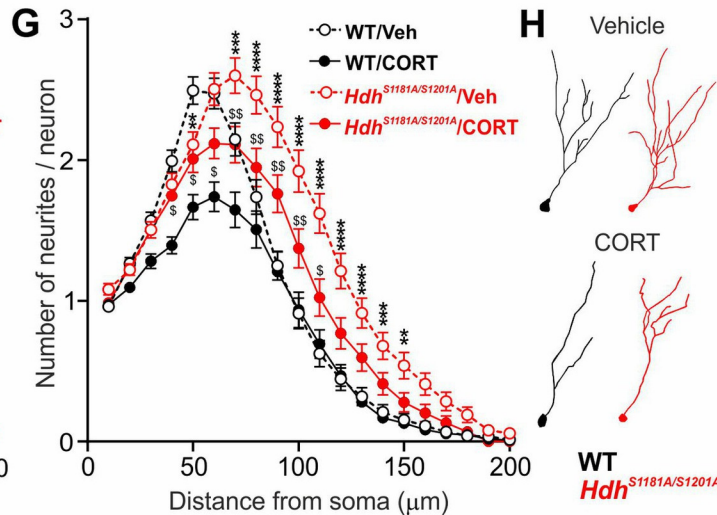
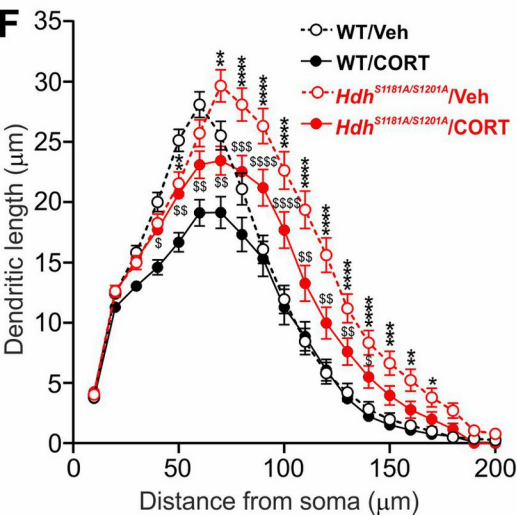
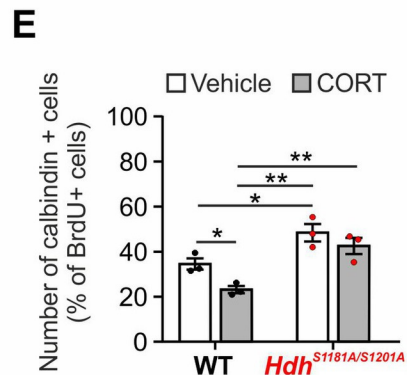
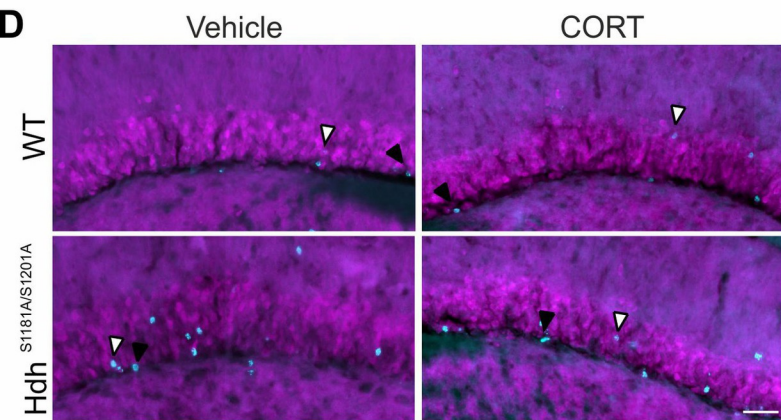
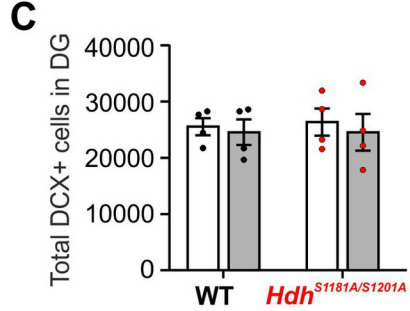
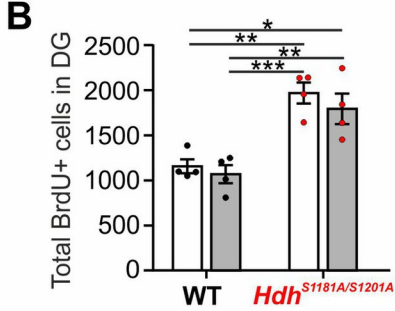
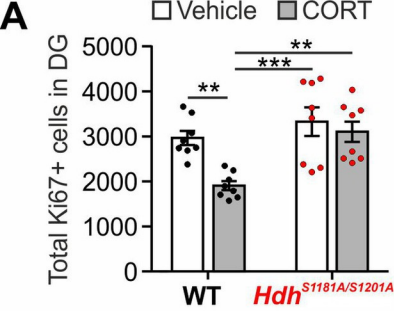


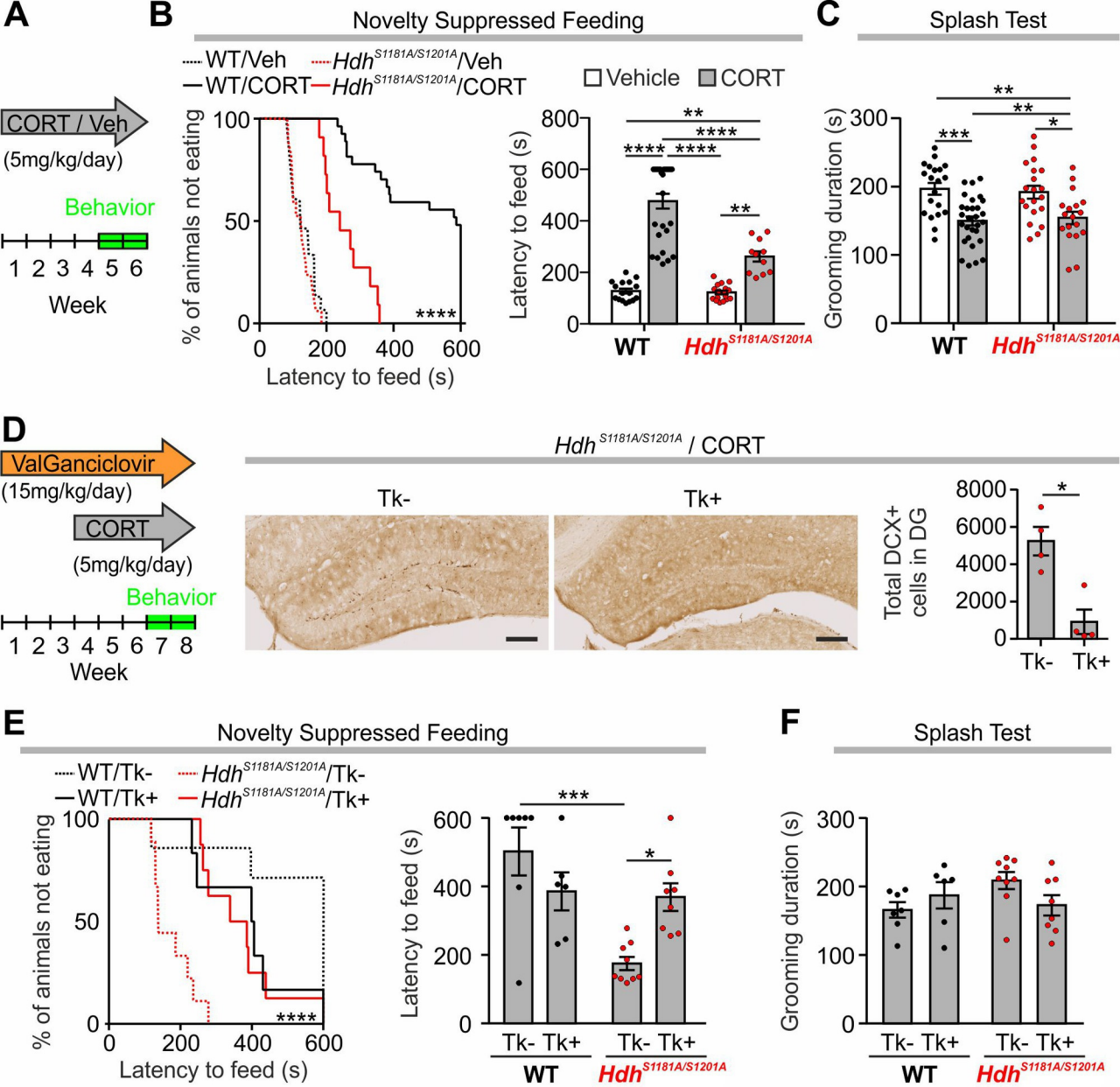


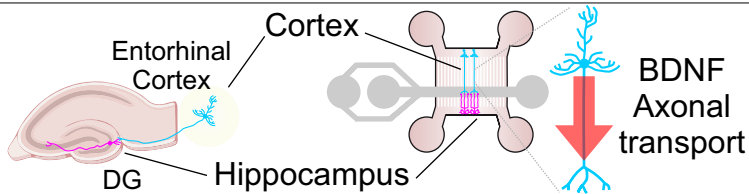


□ Vehicle ■ CORT





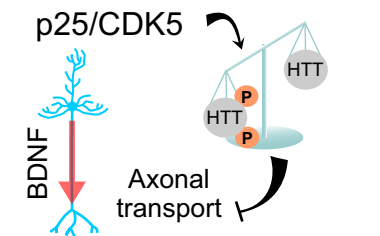
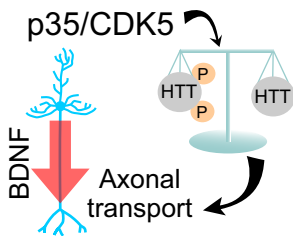




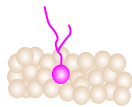
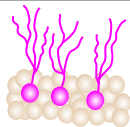
Control

Chronic Corticosterone

Cortical axons



DG



↓ Decreased neurogenesis

Behavior



↑ Increased depression related behaviors